JOURNAL OF Applied Polymer SCIENCE

Self-Segregating Hyperbranched Polymer/Silver Nanoparticle Hybrids in Thermoplastic Polyurethane Films

Joshua A. Orlicki, Nicole E. Zander, George R. Martin, Wendy E. Kosik, J. Derek Demaree, Julia L. Leadore, Adam M. Rawlett

United States Army Research Laboratory, 4600 Deer Creek Loop, Aberdeen Proving Ground, Maryland 21005

Correspondence to: J. A. Orlicki (E-mail: joshua.a.orlicki.civ@mail.mil)

ABSTRACT: Self-segregating hyperbranched polymer (HBP) additives have been utilized to concentrate silver nanoparticles (AgNPs) at the air interface of polyurethane films. The limited spontaneous surface migration of the AgNPs was enhanced through the addition of appropriately functionalized HBPs. Both amine and thiol terminated additives were employed to allow interaction of the HBP with the nanoparticles. Both types of additives increased surface concentration of silver modestly, though the thiol-terminated HBPs demonstrated nearly a seven-fold enhancement of surface migration. It was also found that wholly-aliphatic HBPs demonstrated only slightly reduced ability to bias AgNP concentration as compared to HBPs functionalized with perfluorinated chains. In addition, films containing 1% total silver concentration were tested for antimicrobial activity using the ASTM-E 2180 protocol. Significant reduction of the microorganisms was observed for all samples, 6-log reduction was achieved for the gram-negative bacteria *P. aeruginosa*, the gram-positive bacteria *S. aureus*, and the fungi *C. albicans*. © 2012 Wiley Periodicals, Inc.† J. Appl. Polym. Sci. 000: 000–000, 2012

KEYWORDS: nanoparticles; nanowires; nanocrystals; films; dendrimers; hyperbranched polymers; macrocycles; surfaces; interfaces

Received 26 July 2012; accepted 19 September 2012; published online
DOI: 10.1002/app.38620

INTRODUCTION

The advent of inexpensive analytical methods to characterize nanoscale materials has led to an explosion in the study of nanoparticles of widely varying composition.[1–5] They are of interest for their intrinsic properties, and also as components in nanocomposite applications. Potential applications range from physical reinforcement to sensing applications to controlling optical properties with high fidelity.[6–10] Reactive substrates are also of interest, and noble metal particles have recently been reviewed for application to the purification of drinking water.[11] Perhaps most promising, the tools of self-assembly can be employed to direct nanoparticles to a specific phase of a composite material. This has been demonstrated in several block copolymer systems,[12–16] where functionalized nanoparticles preferentially equilibrate either at the phase interface or in a preferred phase. Complimentary work has also demonstrated the preparation of responsive systems, employing thermally labile ligands to control distribution in a blocky polymer system.[17,18] Nanocomposite hydrogels have also been prepared, taking advantage of both phase segregation and filler content to achieve physical reinforcement.[19] These approaches have largely dealt with particulate distribution in the bulk of composites, but control over additive distribution would afford additional opportunity for the design of high-efficiency functional materials, especially with respect to control over composite surface properties. If active particles could be biased to concentrate at a composite surface, then a reduced total loading would be required to functionalize the composite surface, the mass-transport limitations could be minimized, and the particle impact on the bulk properties of the composite could be minimized.

Silver nanoparticles have been studied extensively, and have been synthesized by a number of elegant routes.[20–24] In addition, their synthesis has been templated using dendrimeric materials, leading to hybrid organic/inorganic particles.[1,2,25–27] In composite applications they are frequently used to impart conductivity by loading above the percolation threshold, or to enhance sensitivity of a surface using enhanced Plasmon resonance.[8,28,29] They may also impart antimicrobial characteristics, as silver has long been known as a broad-spectrum antimicrobial agent, which functions through the slow release of ions to its environment.[30–39] Recent reports have highlighted their activity as potential antiviral agents as well,[40] as well as their use specifically in antimicrobial coatings;[41] a book providing an overview of nanosilver applications was recently published.[42]

Applied Polymer SCIENCE

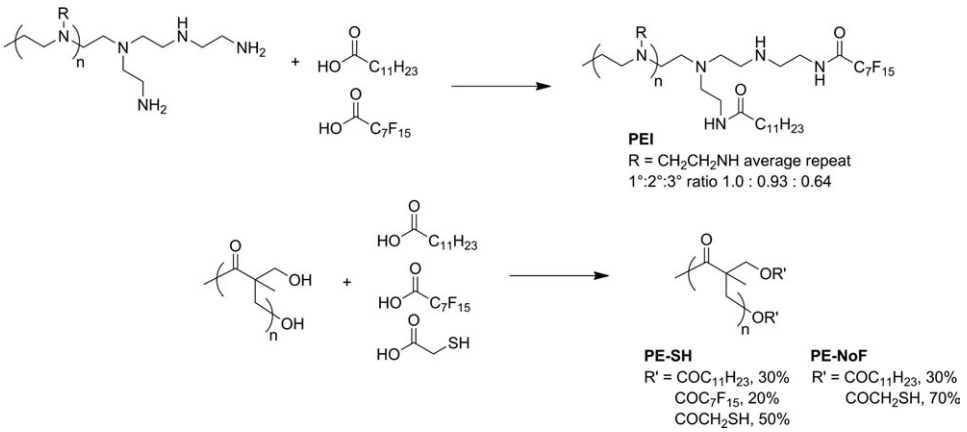

Scheme 1. Synthetic approach to modify commercially available hyperbranched polymer cores. Polyethyleneimines were amidated through the azeotropic removal of water. Polyesters were reacted in the melt under constant N_2 purge to ensure good conversion.

The current investigation seeks to employ polyfunctional ligands to control the distribution of nanoparticles in a cast film. The ligands in this case are based on hyperbranched polymers (HBP), which have a rich history of utility when used as additives to linear polymer systems. Several excellent reviews on the general properties, modification, and assembly of relevant HBPs have been published recently.[43–45] The authors have previously demonstrated effective migration of polyetherimide-based HBPs to a film surface,[46] and have since demonstrated the transport of polyoxometallates to a polyurethane surface using modified commercially available polyethyleneimine (PEI) HBPs.[47] There is also precedent for using similar HBPs to control the distribution of silver nanoparticles in an electro-spun fiber,[48] to stabilize silver nanoparticles for use in a transparent antimicrobial film[49]; a recent review highlighted strategies to form nanohybrid materials with HBPs.[50] In the current study, polyurethane films were cast, which incorporated a fixed quantity of silver nanoparticles stabilized with oleylamine ligands. This baseline material was compared to polyurethane films combining silver nanoparticles mixed with HBP-based ligands, and the resultant variation of surface distribution was examined. The HBP-based additives were found to increase surface concentrations of silver.

EXPERIMENTAL

Materials

A HBP (Boltorn H20) with an average molecular weight of 2000 Da was obtained from Perstorp Corporation. For purposes of stoichiometry determination, a repeat unit mass of 114.1 g/OH was used, which neglected end group loss due to cyclization. Hyperbranched PEI (Lupasol g20wf) with an average molecular weight of 1300 Da, an amine ratio of primary(1°, terminal group):secondary (2°, linear segment):tertiary (3°, branch point) of 1.0 : 0.91 : 0.64, and an equivalent weight of 110 g/1° amine was obtained from BASF. The thermoplastic polyurethane substrates (TPU) were cast from Noveon (Estane 58237, T_g −24°C), a TPU designed for improved moisture transport properties. Perfluorooctanoic acid (PFOA) was purchased from Exfluor Reseach Corporation. All other chemicals were purchased from Sigma-Aldrich or Alfa-Aesar and used as received.

Methods

Hyperbranched Polymer Modification. Hyperbranched polymers were obtained from commercial sources and modified using the methods shown in Scheme 1. The hyperbranched PEIs were amidated via an acid catalyzed condensation reaction with a Dean Stark trap in refluxing toluene to drive conversion via the azeotropic removal of evolved water. The PEI (10 g, 90.9 mmol 1° amine) was dissolved in 50 mL refluxing toluene, and lauric acid (0.2 eq. relative to 1° amine content, 18.2 mmol, 3.64 g) was added. After about 30 min, PFOA (0.2 eq. relative to 1° amine content, 18.2 mmol, 7.53 g) was added and the solution was allowed to react overnight. The product was dried via rotary evaporation without further purification. The modified HBPs were characterized with ^{1}H and ^{13}C NMR and GPC. The NMR analyses were carried out on a Bruker 600 MHz Avance spectrometer. Chemical shifts were referenced to the residual solvent peak ($CDCl_3$, 7.26 ppm for ^{1}H, 77.36 for ^{13}C); integrations were based off of the methyl group of the aliphatic chain end for the ^{1}H spectra. ^{1}H NMR (600 MHz, $CDCl_3$) δ 8.11 (0.1 H), 7.20 (0.1 H), 7.12(0.1 H, amide protons), 3.61 (0.3 H), 3.28, 3.22, 3.14, 3.08 (3.1 H, amide CH_2, PEI side), 2.75, 2.68, 2.62, 2.49 (42 H, backbone CH_2), 2.11 (2H, aliphatic CH_2 α to amide), 1.55 (2H, aliphatic CH_2 β to amide), 1.19 (17 H, aliphatic CH_2), 0.82 (3H, aliphatic CH_3). ^{13}C NMR (151 MHz, $CDCl_3$) δ 181.19 (aliphatic CO), 173.74 (mercapto acetic CO), 161.95 (PFOA CO), 129.26, 128.45, 125.52, 100.26 (CF_2, CF_3), 54.54, 52.44, 49.47, 47.61 (backbone CH2), 41.64, 39.21 (CH_2 α to amide, PEI side), 36.87(CH_2 α to amide, aliphatic side), 32.15, 29.88, 29.59, 27.10 (CH_2 aliphatic) 26.14 (aliphatic CH_2 β to amide, aliphatic side), 22.90 (CH_2 alpha to methyl group), 14.38 (aliphatic CH_3). Size measurements using triple-detector gel-permeation chromatography were attempted, but there was insufficient refractive index signal in THF solvent; in toluene the polymer appeared to be present solely as high molecular weight aggregates. FTIR analysis, major peaks listed in wavenumbers (cm^{-1}): 3251 (H-bonding of amine), 2923, 2850 (aliphatic CH stretching), 1683, 1645, 1653 (carbonyl peaks), 1558, 1239, 1205, 1146.

Polyester HBPs were functionalized using a modified melt condensation procedure.[51] The base PE-polyol (2.31 g, 20.3 mmol

—OH) was melted at ca 150°C under a nitrogen purge and then combined with lauric acid (0.3 eq., 1.2 g) and PFOA (0.2 eq., 1.70 g). A few milligrams of *p*-toluenesulfonic acid were added to catalyze the reaction. Mercaptoacetic acid (0.5 eq., 0.92 mL) was added and the mixture was allowed to react for about 4 h under a constant flow of nitrogen. The solution was then allowed to cool to room temperature and dried under nitrogen. The modified HBPs were characterized with ^{1}H and ^{13}C NMR and GPC. The NMR analyses were carried out on a Bruker 600 MHz spectrometer. Chemical shifts were referenced to the residual solvent peak ($CDCl_3$, 7.26 and 77.36 ppm for ^{1}H and ^{13}C, respectively). For the PE-SH polymer, integrations were based off of the aliphatic methyl group of the lauric acid. ^{1}H NMR (600 MHz, $CDCl_3$) δ 5.23, 4.25(11 H, backbone CH_2), 3.70, 3.61, 3.52, 3.43 (7.8 H, backbone CH_2), 3.27 (3.3 H, CH_2 of thiol), 2.29 (2H, aliphatic CH_2 α to ester), 2.03 (1.6 H, —SH), 1.56 (2H, aliphatic CH_2 β to ester), 1.23 (27H, aliphatic CH_2 and backbone CH_3), 0.86 (aliphatic CH_3). ^{13}C NMR (151 MHz, $CDCl_3$) δ 175.03, 173.65, 172.09, 170.77 (carbonyls), 71.32, 70.75, 69.47, 69.20, 66.27, 65.08 (backbone CH_2's), 48.92, 46.89 (quaternary carbons in backbone), 34.83, 34.36, 34.17, 32.21, 29.92, 29.79, 29.65, 29.44 (aliphatic CH_2 end groups), 26.58, 25.15(CH_2 from SH), 23.00 (α to CH_3 of aliphatic end group), 18.08, 17.64,(backbone CH_3) 14.45 (aliphatic chain end CH_3). GPC analysis (THF) Mn 26.1 kDa, Mw 33.1 kDa (1.3 PDI). FTIR analysis, major peaks listed in wavenumbers (cm^{-1}): 3504 (H-bonding), 2904, 2851 (aliphatic CH stretching), 2563 (—SH), 1717 (carbonyls-broad), 1457, 1280–1107.

For the PE-NoF polymer, integrations were based off of the aliphatic methyl group of the lauric acid. ^{1}H NMR (600 MHz, $CDCl_3$) δ 4.25(11.7 H, backbone CH_2), 3.70, 3.62, 3.54, 3.43 (8.4 H, backbone CH_2), 3.27 (3.2 H, CH_2 of thiol), 2.28 (2 H, aliphatic CH_2 α to ester), 2.02(1.5 H, —SH), 1.56 (2H, aliphatic CH_2 β to ester), 1.23 (27H, aliphatic CH_2 and backbone CH_3), 0.86 (3H, aliphatic CH_3). ^{13}C NMR (151 MHz, $CDCl_3$) δ 174.65, 174.26, 173.65, 172.07, 171.27, 170.77 (carbonyls), 71.34, 70.80, 69.48, 69.12, 66.32, 65.39, 64.98 (backbone CH_2), 48.95, 46.87 (quaternary carbon backbone), 34.81, 34.34, 34.15, 32.20, 29.91, 29.78, 29.64, 29.43 (aliphatic CH_2 end groups), 26.59, 25.14 (CH_2 of thiol), 22.99 (α to CH_3 of aliphatic end group), 18.07, 17.65 (backbone CH_3), 14.45 (aliphatic chain end CH_3). GPC analysis (THF) Mn 9.1 kDa, Mw 13.5 kDa (1.5 PDI). FTIR analysis, major peaks listed in wavenumbers (cm^{-1}): 3506 (weak), 2923, 2852 (aliphatic CH stretching), 2561(weak, —SH), 1652, 1457, 1280, 1231, 1131.

Silver Nanoparticle Preparation. Organic solvent soluble silver nanoparticles were synthesized via literature procedure.[20] Silver acetate in toluene was reduced in the presence of oleylamine to form monodisperse silver nanoparticles. Typically, 0.1 g of silver acetate was dissolved in 4 g of oleylamine and then added to 100 mL of refluxing toluene in order to synthesize 7–9 nm particles. After ~18 h, the solution was cooled to room temperature, most of the solvent was removed and the particles were purified by precipitation into methanol. After centrifugation, the liquid was decanted and the particles were redissolved into hexanes, reprecipitated into methanol twice, and then dried and stored in a vacuum desiccator.

Film Preparation. Cast films were prepared, beginning with stock solutions of the linear polymer TPU (Estane 58237) at about 30 mg/mL, and stock solutions of the additives at about 3 mg/mL. The stock solutions were then combined in appropriate quantity to yield solutions containing ~0.5–4% additive based on the solids weight. For AgNP-HBP composites, stock solutions of the HBP and the AgNP were combined for about 45 min prior to their addition to the TPU solution, permitting time for ligand exchange prior to dilution. The solutions were cast onto glass slides and the solvent evaporated slowly in a semisaturated atmosphere.

Surface Analysis. X-ray photoelectron spectroscopy (XPS) data was obtained using a Kratos Axis Ultra X-ray photoelectron spectroscopy system, equipped with a hemispherical analyzer. A 100 W monochromatic Al Kα (1486.7 eV) beam irradiated a 0.5 $\times$ 1.0 mm^2 sampling area. Survey scans were taken at pass energy = 80 eV. Elemental high resolution scans for C 1 *s*, O 1 *s*, N 1 *s*, Ag 3 *d*, S 2 *p*, and F 1 *s* were taken at pass energy = 20 eV. CasaXPS software was utilized for all data analysis. In instances where Si was detected, it was attributed to SiO_2 contamination or pinholes in the film, so the Si value was disregarded and the corresponding oxygen signal was corrected by an appropriate amount (e.g., reduced O 1 *s* signal by twice the Si measured); the values presented in Tables I–III were normalized to 100% using this correction factor. Contact angles were recorded using a goniometer equipped with a CCD camera and an image capture program employing LabView software. Contact angles were measured by defining a circle about the drop, and recording the tangent angle formed at the substrate. The LabView program measures this angle on the left and right sides of the snapshot, and then averages them for a final contact angle value. Atomic force microscopy (AFM) was used to determine the nanoparticle size and images were obtained on a Dimension 3100 AFM equipped with a Nanoscope IV scanning probe microscope controller. Commercial AFM Tips (RTESPA from Veeco) were used as received.

Antimicrobial Analysis. The antimicrobial efficacy of the surfaces was examined against *P. aeruginosa*, *S. aureus*, and *C. albicans* using a standard test method (ASTM E-2180) for non-leaching hydrophobic materials. TPU films were cast onto standard microscope slides cut in half, resulting in a film surface area of 1.5 $inch^2$ (9.4 cm^2). Briefly, 1 $\times$ 10^6 cells in agar slurry were loaded onto the test surface (ca. 10 μm thick coating) and incubated at 37°C for 24 h. The inoculum was recovered in a neutralizing medium of Dey Engley Broth via sonication and vortexing. The broth was diluted with 0.85% saline water and plated. Colonies were counted after 48 h and treated samples were compared to controls incubated on the native TPU. Further details can be found in the ASTM E-2180 specifications.[52] An analogous test conducted in a 25-well plate (1 cm^2 of film) was recently reported in the literature.[53]

RESULTS AND DISCUSSION

Commercially available hyperbranched PEI and PE were obtained from BASF and Perstorp, respectively. The chain ends of these polymers were modified according to Scheme 1. Both

Table I. PE Series Film Composition (XPS Atomic %)

Composition	Ag	C	F	N	O	S
TPU	0.00	81.90	0.00	2.33	15.78	0.00
1% AgNP	1.02	82.70	0.00	1.29	14.99	0.00
0.5% PE-SH	0.00	67.46	12.62	1.64	17.31	0.97
1% PE-SH	0.00	68.79	14.01	1.18	14.61	1.41
2% PE-SH	0.00	63.40	17.36	0.82	17.24	1.18
3% PE-SH	0.00	65.86	15.36	0.82	16.48	1.49
4% PE-SH	0.00	64.91	16.48	0.67	16.58	1.37
1% AgNP 0.5% PE-SH	6.91	72.90	0.88	0.00	18.24	1.08
1% AgNP 1% PE-SH	5.46	70.17	4.37	0.00	18.06	1.95
1% AgNP 2% PE-SH	2.22	66.10	9.36	0.00	20.34	1.98
1% AgNP 3% PE-SH	2.21	65.21	11.43	0.00	18.71	2.43
1% AgNP 4% PE-SH	1.50	61.84	16.21	0.00	18.53	1.93

backbones were fractionally functionalized using PFOA and lauric acid. The PEI was functionalized in refluxing toluene, using the azeotropic removal of water to simultaneously dry the polymer and drive the reaction equilibrium to yield a viscous oil as the product. Functionalization of the PE occurred in the melt, neat at about 150–160°C under a constant N_2 purge. After the PFOA and lauric acids had been homogenized into the melt and allowed about 1 h to react, mercaptoacetic acid was added in order to install groups capable of chelating silver. The polymers were used without further purification after modification. It is recognized that the reaction conditions selected for the PE modification will lead to significant transesterification. Differentiating backbone segments that corresponded to branches, "linear" segments, or chain ends was not possible, given the similarity of the backbone and end group chemistries. The resulting materials were characterized using NMR spectroscopy and gel permeation chromatography. In addition to the PFOA/lauric acid/thiol terminated polyester sample (PE-SH), one composition was prepared, which contained no PFOA but maintained the lauric acid and thiol chain ends (PE-NoF).

Silver nanoparticles (AgNPs) were prepared according to a literature procedure.[20] Nanoparticle size was evaluated by AFM (Figure 1). Samples for AFM analysis were prepared by casting a small amount of dilute hexane solution of sonicated silver nanoparticles onto a glass cover slip. Films were air dried and examined in tapping mode; the average particle size determined by AFM height section analysis was 8 ± 1.5 nm.

Silver nanoparticle composites were then prepared using a low T_g (−24°C) thermoplastic polyurethane (TPU, Estane 58237) as the matrix polymer, cast as films from THF. Formulations for the desired film compositions were prepared by first combining the appropriate HBP solution volume in a vial, followed by AgNP solution to yield the desired ratio of AgNP to HBP. These were incubated about 45 min at room temperature without agitation, and then the matrix polymer solution was added, such that the total AgNP loading was 1% of total solids. Films were cast onto microscope cover slips and dried in a covered petri dish placed in a nitrogen-purged cabinet. Reducing the rate of solvent evaporation diminished the occurrence of drying defects and minimized the impact of ambient humidity variations, which can lead to breathe figure formation during film drying if uncontrolled.[54] The resulting films were clear in the absence of AgNP, and maintained clarity with a light brown tint with the inclusion of the nanoparticles.

Table II. PE-NoF Series Films Composition (XPS Atomic %)

Composition	Ag	C	N	O	S
0.5%PE-NoF	0.00	78.30	1.84	18.94	0.92
1%PE-NoF	0.00	77.68	0.73	20.52	1.06
2%PE-NoF	0.00	78.36	1.35	19.17	1.11
3%PE-NoF	0.00	77.67	1.58	19.68	1.07
4%PE-NoF	0.00	76.30	1.01	21.07	1.62
1%AgNP 0.5%PE-NoF	5.12	71.88	1.15	20.67	1.18
1%AgNP 1%PE-NoF	3.35	73.29	1.05	20.90	1.41
1%AgNP 2%PE-NoF	3.74	71.46	0.00	22.45	2.35
1%AgNP 3%PE-NoF	3.48	71.11	0.00	22.49	2.92
1%AgNP 4%PE-NoF	2.20	72.31	0.00	22.66	2.83

Table III. PEI Series Film Compositions (XPS Atomic %)

Composition	Ag	C	F	N	O
0.5%PEI	0.00	69.52	7.10	7.50	15.89
1%PEI	0.00	66.90	10.10	7.69	15.31
2%PEI	0.00	66.54	11.33	7.52	14.61
3%PEI	0.00	62.27	14.63	13.12	9.99
4%PEI	0.00	63.82	13.67	10.51	12.01
1%AgNP 0.5%PEI	2.02	65.67	13.82	9.49	9.00
1%AgNP 1%PEI	1.04	68.27	12.50	7.71	10.48
1%AgNP 2%PEI	1.11	60.27	20.10	9.76	8.76
1%AgNP 3%PEI	1.00	66.40	12.63	8.75	11.21
1%AgNP 4%PEI	1.27	61.94	18.69	10.33	7.77

The AgNP concentration was held constant at 1% of total solids, while the HBP additive ranged from 0.5 to 4.0% total solids. These films were then interrogated using surface analysis techniques such as water contact angle analysis and XPS. Given the low glass transition temperature of the TPU matrix, it was accepted that the films were essentially annealed when stored at room temperature, reducing the occurrence of kinetically trapped film structures.

Contact angle is the more qualitative technique of the two, but provides some insight into the surface characteristics of the resultant films (Figure 2). The base TPU exhibited a water contact angle of about 66° (±2.1), which reflects the influence of the hydrophilic alcohols used as chain extender in the preparation of the TPU. The same film doped with 1% AgNP (wt/wt) became slightly more hydrophobic, increasing the contact angle to about 70° (± 1.4). The behavior of the three types of HBP is in line with our expectations. The PE HBP exhibited the highest contact angle, owing to its modestly hydrophilic backbone and PFOA/laurate chain ends that exhibit greater influence than the thiol groups. The PE-NoF was less hydrophobic in the absence of the PFOA groups, but still exhibited an increase in hydrophobicity relative to the base TPU. The PEI exhibited a small increase in hydrophilicity at low concentrations, although the effect scaled with additive concentration. It should be noted that this effect is more modest than the one we have reported previously.[47] In the current study, the method of end group modification has changed, employing amidation to functionalize the chain ends instead of epoxy-amine and vinyl-amine bond formation. The resultant polymer was less hydrophilic overall, and the additive exhibited a reduced impact upon cast films incorporating the additive.

The mixture of AgNPs with HBPs led to hybrid particles that altered film characteristics in a combination of both additive constituents. In the instance of films containing the PE-based HBP complexes, a similar contact angle was observed as compared to films containing the HBP alone. The contact angle was slightly reduced for the PE-SH/AgNP system and almost maintained the values observed for the PE-NoF/AgNP samples. In the case of the PEI/AgNP systems, the change was more dramatic, increasing hydrophobicity relative to the base material. The impact of the AgNP incorporation was reduced as the ratio of HBP to AgNP was increased, yielding surface properties that more closely track those of the polymer additive by itself.

XPS was used to characterize the surface elemental composition as a function of additive composition and loading. Tables I–III capture the data for these compositions, and allow for the quantitative comparison of each formulation.

Table I provides reference values for the base TPU, for the base TPU doped with 1% (total solids basis) of silver nanoparticles,

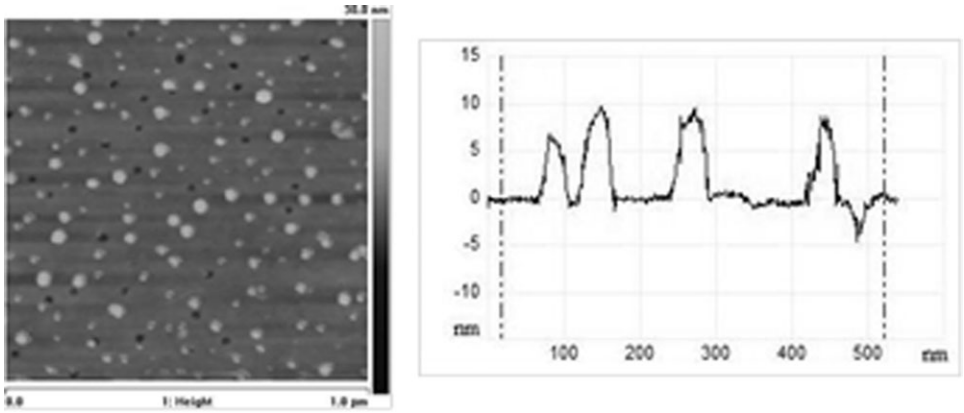

Figure 1. AFM image of AgNP's prepared according to literature procedure. Average particle size about 8 ± 1.5 nm.

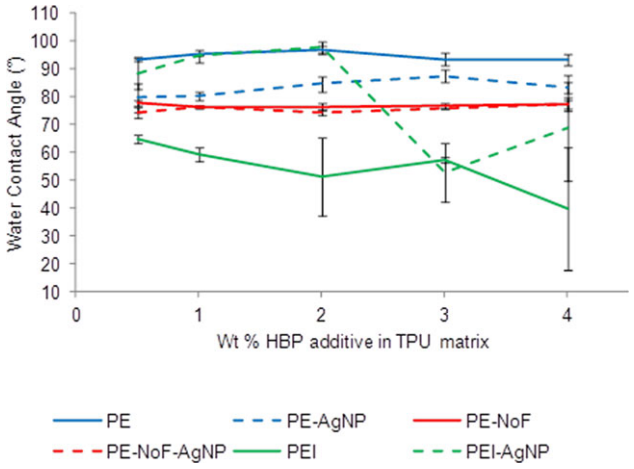

Figure 2. Contact angle as a function of additive concentration in TPU cast films. Additive loading expressed as % total solids; all AgNP samples include 1% AgNP on total solids basis.

and the corresponding series of films prepared with the PE-SH additive. The amount of silver at the surface for the reference AgNP sample was comparable to the quantity incorporated into the material, and although the ligand of the AgNP was an amine, the net nitrogen levels at the surface dropped to about 1%. The behavior of the PE-SH additive series is substantially different from the AgNP reference and baseline TPU. It is clear from both the fluorine and sulfur levels that the HBP efficiently migrated to the film surface, which also caused a concurrent decrease in C, O, and N levels. The impact of the additive is also apparent for the samples which actually incorporate AgNPs, which resulted in a marked increase in Ag at the surface of the films. The silver exhibited a nearly seven-fold improvement in surface migration due to the HBP additive. The perturbation in surface fluorine levels also suggests that the HBP is partially displacing the oleylamine ligands of the AgNPs, but the remaining ligands lead to a dramatic reduction (dilution) in the level of fluorine at the surface relative to the films cast with only the HBP additive. This effect is ameliorated as the relative loading of the HBP increases, and the fluorine level more closely mirrors that of the native HBP films.

The maximum level of Ag at the film surface was observed with the 0.5 PE-SH loading, and the observed level of silver diminished as the amount of HBP increased. That the maximal amount of silver was observed at the lowest loading level of HBP suggests that the silver is the limiting species when the interaction of the AgNP and HBP is considered. At the lowest HBP loading, the silver loading per additive is greatest. As additional HBP is introduced to the system, the Ag attached to each HBP on average is reduced. If the HBP had been the limiting species at the lowest loading, a maximal amount of silver at the surface would have been observed in one of the samples with a greater HBP : AgNP ratio.

Table II reflects the composition of films prepared with a PE-based HBP absent any fluorine modification. It was hypothesized that, given the high levels of surface migration observed with the 1Ag0.5PE sample and the diminution of the surface fluorine levels that a wholly aliphatic HBP may serve in a similar fashion. This hypothesis was largely borne out by the data presented here, where the 1Ag0.5PE-NoF sample was effective at promoting migration of the AgNP, resulting in about five-fold increase. However, the fluorine-functionalized additive demonstrated a greater ability to bias surface concentration of the AgNP. Given the wholly aliphatic nature of Pe-NoF, this additive may still be preferable to bias surface concentration of AgNP's if concerns regarding the use of perfluorinated components preclude their use as HBP end groups.

The final table of XPS data (Table III) provides insight into the action of the PEI-based additives in the TPU matrix system. The PEI is less effective than the PE-based additives at promoting AgNP concentration at the air-polymer interface, although the uncomplexed additive is clearly effective at migrating to the film surface (as demonstrated by the fluorine levels and relative increase in nitrogen relative to the TPU baseline). The PEI has yielded a two-fold enhancement in AgNP migration. It is important to consider the nature of the HBP interaction with the AgNP. The PEI has primary amine chain ends, as well as secondary/tertiary amines in the polymer backbone, which could potentially interact with the AgNP. It is unlikely, though, that these interactions are substantially more favorable than the as-prepared AgNP ligand of oleylamine. When the nature of the interaction is considered, it appears that the PE-based systems with their thiol chain ends are more effective at displacing the oleylamine ligands and may form much stronger bonds with the AgNP.

Biological activity for a selection of films was assayed, including the TPU control, a 1% AgNP sample, and the 1AgNP0.5PE-SH and 1AgNP0.5PEI films. The films were evaluated using the ASTM E2180 method, which was developed specifically as an assay for films. The test introduces a microbial challenge to the film in an agar support for 24 h contact, at which time the agar is removed and any remaining cells are grown to probe activity. This method was applied using a selection of organisms as the microbial challenge, including gram-negative bacteria *P. aeruginosa*, the gram-positive bacteria *S. aureus*, and the fungi *C. albicans*. In all cases the AgNP as well as the HBP-AgNP doped films exhibited sufficient activity to achieve 6-log kill. While the XPS and data suggests a greater amount of active silver should be at the surface of the film for the HBP-AgNP doped films, the assay available to us lacks the resolution to differentiate between the base AgNP and our desired formulations; the assay can only confirm that the HBP-AgNP particles retain antimicrobial efficacy. It is recognized that the antimicrobial action of silver is dependent upon the release and diffusion of ions from the surface, and the TPU matrix exhibited some swelling in the presence of agar during the microbial challenge. As such, this matrix was not ideal to determine the retention of additives in an aqueous environment, but the segregation of the additives in the matrix should be representative of performance in many polar thermoplastic systems, and this approach affords a new mechanism of maximizing additive concentration at a film surface.

CONCLUSIONS

Hyperbranched polymer based additives were used to bias the distribution of silver nanoparticles in a thermoplastic

polyurethane film. A series of commercially available HBPs were modified with low surface energy chain ends to promote their migration to a film surface in a polyurethane matrix. The additives were incubated with pre-formed silver nanoparticles, and were then combined with the polyurethane and cast as films. The HBP-AgNP containing films exhibited increased quantities of silver at the film surface relative to the AgNP control. When measured using XPS, the HBP-AgNP's exhibited a nearly seven-fold increase in silver near the surface. A strong dependence was found on the method of interaction of the additive with the AgNP, whereby the thiol-terminated HBPs exhibited substantial surface enrichment (4–7 fold) at low loading levels (0.5% wt/wt); the PEI-based additive only showed about two-fold enhancement of Ag at the surface (0.5% wt/wt). Surprisingly, the HBP additive that lacked perfluorinated chain ends to drive surface segregation exhibited a substantial level of surface segregation (ca. five-fold). All of the resultant films were assayed for antimicrobial activity against a range of microbial challenges [gram (−), gram (+), fungus] and all exhibited 6-log antimicrobial activity over a 24 h period.

ACKNOWLEDGMENTS

This research was supported in part through an appointment to the Postgraduate Research Participation Program at the U.S. Army Research Laboratory administered by the Oak Ridge Institute for Science and Education through an interagency agreement between the U.S. Department of Energy and USARL. It was also conducted with the support from the Director's Research Initiative. The authors would like to thank BASF and Perstorp for their generous donation of materials.

REFERENCES

1. Scott, R. W.; Wilson, O. M.; Crooks, R. M. *J. Phys. Chem. B* **2005**, *109*, 692.
2. Crooks, R. M.; Zhao, M.; Sun, L.; Chechik, V.; Yeung, L. K. *Acc. Chem. Res.* **2001**, *3*, 181.
3. Niederberger, M.; Garnweitner, G. *Chem. Eur. J.* **2006**, *12*, 7282.
4. Kotlyar, A.; Perkas, N.; Amiryan, G.; Meyer, M.; Zimmerman, W.; Gedanken, A. *J. Appl. Polym. Sci.* **2007**, *104*, 2868.
5. Liu, J.-F.; Yu, S.-J.; Yin, Y.-G.; Chao, J.-B. *Trends Anal. Chem.* **2012**, *33*, 95.
6. Lim, S. I.; Zhong, C.-J. *Acc. Chem. Res.* **2009**, *42*, 798.
7. Chatterjee, U.; Jewrajka, S. K.; Guha, S. *Polym. Compos.* **2009**, *30*, 827.
8. Khlebtsov, N. G.; Dykman, L. A. *J. Quant. Spectrosc Radiat. Transfer.* **2010**, *111*, 1.
9. Holder, E.; Tessler, N.; Rogach, A. L. *J. Mater. Chem.* **2008**, *18*, 1064.
10. Liu, Z.; Luo, L.; Dong, Y.; Weng, G.; Li, J. *J. Colloid Interface Sci.* **2011**, *363*, 182.
11. Pradeep, T.; Anshup. *Thin Solid Films* **2009**, *517*, 6441.
12. Lin, Y.; Boker, A.; He, J. B.; Sill, K.; Xiang, H. Q.; Abetz, C.; Li, X. F.; Wang, J.; Emrick, T.; Long, S.; Wang, Q.; Balazs, A.; Russell, T. P. *Nature* **2005**, *434*, 55.
13. Balazs, A. C.; Emrick, T.; Russell, T. P. *Science* **2006**, *314*, 1107.
14. Warren, S. C.; Messina, L. C.; Slaughter, L. S.; Kamperman, M.; Zhou, Q.; Gruner, S. M.; DiSalvo, F. J.; Wiesner, U. *Science* **2008**, *320*, 1748.
15. Darling, S. B. *Prog. Polym. Sci.* **2007**, *32*, 1152.
16. Alexandridis, P.; Tsianou, M. *Eur. Polym. J.* **2011**, *47*, 569.
17. Costanzo, P. J.; Demaree, J. D.; Beyer, F. L. *Langmuir* **2006**, *22*, 10251.
18. Costanzo, P. J.; Beyer, F. L. *Macromolecules* **2007**, *40*, 3996.
19. Schexnailder, P.; Schmidt, G. *Colloid Polym. Sci.* **2009**, *287*, 1.
20. Hiramatsu, H.; Osterloh, F. E. *Chem. Mater.* **2004**, *16*, 2509.
21. Chen, M.; Feng, Y.-G.; Wang, X.; Li, T.-C.; Zhang, J.-Y.; Qian, D.-J. *Langmuir* **2007**, *23*, 5296.
22. Medina-Ramirez, I.; Bashir, S.; Luo, Z.; Liu, J. L. *Colloids Surf. B: Biointerfaces* **2009**, *73*, 185.
23. Garcia-Barrasa, J.; Lopez-de-Luzuriaga, J. M.; Monge, M. *Cent. Eur. J. Chem.* **2011**, *9*, 7.
24. Prasad, T. N. V. K. V.; Kambala, V. S. R.; Naidu, R. *Curr. Nanosci.* **2011**, *7*, 531.
25. Liu, H.; Wang, H.; Guo, R.; Cao, X.; Zhao, J.; Luo, Y.; Shen, M.; Zhang, G.; Shi, X. *Polym. Chem.* **2010**, *1*, 1677.
26. Shi, X.; Lee, I.; Baker, J. R., Jr. *J. Mater. Chem.* **2008**, *18*, 586.
27. Shau, S.-M.; Chang, C.-C.; Lo, C.-H.; Chen, Y.-C.; Juang, T.-Y.; Dai, S. A.; Lee, R.-H.; Jeng, R.-J. *ACS Appl. Mater. Interfaces* **2012**, 4, 1897.
28. Liu, S.; Tang, Z. *J. Mater. Chem.* **2010**, *20*, 24.
29. Stofik, M.; Stryhal, Z.; Maly, J. *Biosensors Bioelectron.* **2009**, 24, 1918.
30. Morones, J. R.; Elechiguerra, J. L.; Camacho, A.; Holt, K.; Kouri, J. B.; Ramirez, J. T.; Yacaman, M. *J. Nanotechnology* **2005**, *16*, 2346.
31. Lee, D.; Cohen, R. E.; Rubner, M. F. *Langmuir* **2005**, *21*, 9651.
32. Kalayer, O. A.; Comert, F. B.; Hazer, B.; Atalay, T.; Cavicchi, K. A.; Cakmak, M. *Polym. Bull.* **2010**, *65*, 215.
33. Marambio-Jones, C.; Hoeck, E. M. V. *J. Nanopart. Res.* **2010**, *12*, 1531.
34. Varprasad, K.; Mohan, Y. M.; Ravindra, S.; Reddy, N. N.; Vimala, K.; Monika, K.; Sreedhar, B.; Raju, K. M. *J. Appl. Polym. Sci.* **2010**, *115*, 1199.
35. Park, J. T.; Koh, J. H.; Lee, K. J.; Seo, J. A.; Min, B. R.; Kim, J. H. *J. App. Polym. Sci.* **2008**, *110*, 2352.
36. Kalayci, O. A.; Comert, F. B.; Hazer, B.; Atalay, T.; Cavicchi, K. A.; Cakmak, M. *Polym. Bull.* **2010**, *65*, 215.
37. Vasilev, K.; Sah, V. R.; Goreham, R. V.; Ndi, C.; Short, R. D.; Griesser, H. *J. Nanotechnology* **2010**, *21*, 215202 (6pp).
38. Arya, V.; Komal, R.; Kaur, M.; Goyal, A. *Pharmacologyonline* **2011**, *3*, 118.

39. Marambio-Jones, C.; Hoek, E. M. V. *J. Nanopart. Res.* **2010**, *12*, 1531.

40. Galdiero, S.; Falanga, A.; Vitiello, M.; Cantisani, M.; Marra, V.; Galdiero, M. *Molecules* **2011**, *16*, 8894.

41. Knetsch, M. L.; Koole, L. H. *Polymers* **2011**, *3*, 340.

42. Stalmashonak, A.; Graener, H.; Seifert, G. Silver Nanoparticles: Properties, Characterization and Applications; A. E. Welles, Eds.; Nova Science: New York, **2010**; p 383.

43. Zhang, X. *Polym. Int.* **2011**, *60*, 153.

44. Zagar, E.; Zigon, M. *Prog. Polym. Sci.* **2011**, *36*, 53.

45. Peleshanko, S.; Tsukruk, V. V. *J. Polym. Sci. Part B: Polym. Phys.* **2012**, *50*, 83.

46. Orlicki, J. A.; Moore, J. S.; Sendijarevic, I.; McHugh, A. *J. Langmuir* **2002**, *18*, 9985.

47. Orlicki, J. A.; Kosik, W. E.; Demaree, J. D.; Bratcher, M. S.; Jensen, R. E.; McKnight, S. H. *Polymer* **2007**, *48*, 2818.

48. Hunley, M. T.; Harber, A.; Orlicki, J. A.; Rawlett, A. M.; Long, T. E. *Langmuir* **2008**, *24*, 654.

49. Gladitz, M.; Reinemann, S.; Radusch, H.-J. *Marcomol. Mater. Eng.* **2009**, *294*, 178.

50. Hu, X.; Zhou, L.; Gao, C. *Colloid Polym. Sci.* **2011**, *289*, 1299.

51. Malmström, E.; Johansson, M.; Hult, A. *Macromolecules* **1995**, *28*, 1698.

52. ASTM method E2180-07(2012) Standard Test Method for Determining the Activity of Incorporated Antimicrobial Agent(s) In Polymeric or Hydrophobic Materials, is available for purchase from the astm.org web site.

53. Yagci, M. B.; Bolca, S.; Heuts, J. P. A.; Ming, W.; de With, G. *Prog. Org. Coat.* **2011**, *72*, 305.

54. Zander, N. E.; Orlicki, J. A.; Karikari, A. S.; Long, T. E.; Rawlett, A. M. *Chem. Mater.* **2007**, *19*, 6145.